AIAA 94-3210

Supersonic Flight Test Results of a Performance Seeking Control Algorithm on a NASA F-15 Aircraft

John S. Orme and Timothy R. Conners
NASA Dryden Flight Research Center
Edwards, California

30th AIAA/ASME/SAE/ASEE Joint Propulsion Conference
June 27–29, 1994 / Indianapolis, IN

SUPERSONIC FLIGHT TEST RESULTS OF A PERFORMANCE SEEKING CONTROL ALGORITHM ON A NASA F-15 AIRCRAFT

John S. Orme* and Timothy R. Conners**
NASA Dryden Flight Research Center
P.O. Box 273
Edwards, California 93523-0273

Abstract

A model-based, adaptive control algorithm called Performance Seeking Control (PSC) has been flight tested on an F-15 aircraft. The algorithm attempts to optimize performance of the integrated propulsion system during steady-state engine operation. The final phase of a 3-year PSC flight test program is described in this paper. Previous studies of use of PSC on the F-15 airplane show improvement in propulsion system performance. Because these studies were conducted using one of two F-15 engines, the full effect on aircraft performance was not measured. During the most recent studies, both engines were optimized to demonstrate the full effect of PSC propulsion system optimization on aircraft performance. Results were gathered over the 1-*g* supersonic envelope demonstrating benefits of the integrated control approach. Quantitative flight results illustrating the PSC method for deriving benefits from the F-15 integrated propulsion system for Mach numbers up to 2 are also presented.

Nomenclature

A/B	afterburner
ADECS	advanced engine control system
AJ	nozzle throat area, in^2
CDP	component deviation parameters
CIVV	compressor inlet variable guide vane angle, deg
DEEC	digital electronic engine control
EAIC	electronic air inlet controller
EPR	engine pressure ratio, *PT6/PT2*
FNP	net propulsive force, lbf
FTIT	fan turbine inlet temperature, °R
HIDEC	Highly Integrated Digital Electronic Control
h_c	capture height, ft
Kf	Kalman filter
MDA	McDonnell Douglas Aerospace, St. Louis, Missouri
NASA	National Aeronautics and Space Administration
N1	fan speed, rpm
N1C2	fan rotor speed, corrected to engine face, rpm
N2	high pressure compressor speed, rpm
PB	burner pressure, lb/in^2
PLA	power level angle, deg
PSC	Performance Seeking Control
PS2	engine face static pressure, lb/in^2
PT2	engine face total pressure, lb/in^2
PT6	augmentor total pressure, lb/in^2
RCVV	rear compressor variable guide vane angle, deg
RDM	rapid deceleration mode
TSFC	thrust-specific fuel consumption, pph/lbf

*Aerospace Engineer. Member AIAA.
**Aerospace Engineer.

TT2 engine face total temperature, °R

VMS vehicle management system

WF core fuel flow, lb/hr

WFAB afterburner fuel flow, lb/hr

Y perpendicular distance the third inlet shock stands from the cowl lip, ft

Prefix

Δ difference

Introduction

Future commercial transports will often fly missions with long cruise legs. Overall system performance will be boosted by using advanced technologies from different disciplines. In the controls field, integration between the propulsion system and the airframe will make significant contributions, particularly for a supersonic transport. Adaptive control is one method of increasing performance of an existing system by reconfiguring the aircraft and propulsion system control effectors. In this manner, aircraft performance may be improved solely by adding control logic.

Digital flight controls, engine controls, and onboard computers allow sophisticated control techniques to be applied to today's advanced aircraft. NASA used one such aircraft, the F-15 Highly Integrated Digital Electronic Control (HIDEC), to explore the potential of such capabilities through flight test application. The integration of engine and airframe control has been the primary objective of the HIDEC program for the last decade. Testing of the Advanced Engine Control System (ADECS) on the F-15 HIDEC demonstrated the advantages of digitally integrated engine and airframe control.[1] The ADECS used flight control information to uptrim the engine pressure ratio (*EPR*) for improved engine performance. Maximum performance *EPR* trims are preprogrammed into onboard schedules. These schedules are developed for the nominal, or average, engine and airframe.

The Performance Seeking Control (PSC) improves upon the ADECS by applying real-time adaptation to the flight-measured article instead of to the nominal engine and airframe.[2, 3] The PSC incorporates inlet, nozzle, stabilator, and adaptive engine models. A Kalman filter (Kf) estimates component deviation parameters (CDP) and provides the primary adaptive feature of the PSC algorithm. The CDP represent the differences between the onboard engine model outputs and measurements. The CDP update the baseline engine model to produce a model that more closely reflects the measured engine performance. Onboard optimization logic searches the models for optimal trim conditions then applies those trims to the engine and airframe system.

Flight testing of the PSC algorithm has been concluded at NASA Dryden Flight Research Center (NASA Dryden). These tests included all of the PSC optimization modes throughout the Mach number and altitude envelope and throttle range. The different optimization modes were demonstrated for single-engine application in subsonic and supersonic flight testing and produced overall engine performance improvements.[4–9] At supersonic conditions, the PSC law optimizes the integrated inlet, stabilator, and engine. For subsonic flight conditions, only the engine is optimized. The stabilator is controlled indirectly through the aircraft pitch rate feedback to offset any disturbances caused by trimming the inlets. Supersonic PSC has increased complexity because controls for the inlet shocks, afterburner, and aircraft stabilator are included. Preliminary analyses show that supersonic PSC realizes performance improvements equal to or greater than those achieved subsonically, especially in the minimum fuel mode.[9]

The last series of flight tests concentrated on the dual-engine application of PSC at supersonic flight conditions. Aircraft performance improvements are directly measurable with dual-engine PSC optimization. Previous research into use of the dual-engine application indicates large benefits in three of the PSC modes and improved acceleration performance.[10] The new rapid deceleration mode (RDM) was also flight tested for the first time. This paper presents quantitative flight results illustrating PSC-derived benefits for propulsion system and aircraft performance for Mach numbers up to 2.

Aircraft Description

The PSC program was implemented on the NASA F-15 research aircraft (fig. 1). This modified high-performance fighter aircraft can achieve speeds in excess of Mach 2. The F-15 aircraft is powered by two F100-derivative afterburning turbofan engines that are given the designation of PW1128 (Pratt & Whitney, West Palm Beach, Florida). The aircraft has been modified with a digital electronic flight control system and is completely instrumented for flight test. Additional information on the F-15 aircraft has previously been reported.[11, 12]

A vehicle management system (VMS) computer, with three channels and three processors per channel, independently hosts the standard F-15 flight control laws and the PSC logic. The VMS computer communicates with other onboard computers through a MIL-STD-1553A multiplexer data bus.[10] The PSC trims are calculated in the VMS computer and transmitted to the engine and inlet controllers through a digital interface and bus control unit. The pilot makes inputs to configure the PSC algorithm and

Figure 1. The NASA F-15 research aircraft.

selects various performance optimization modes using a cockpit control and display panel interface.

Engine Description

The PW1128 engine is a 28,000 lbf thrust class low-bypass ratio, twin spool, afterburning turbofan technology demonstrator, derived from the F100-PW-100 engine.[7] Control effectors include compressor inlet variable guide vane angle, *CIVV*; rear compressor variable guide vane angle, *RCVV*; core fuel flow, *WF*; afterburner fuel flow, *WFAB*; augmentor segment selector valve position; and nozzle throat area, *AJ*. The sensed parameters consist of fan speed, *N1*; high-pressure compressor speed, *N2*; engine face total temperature, *TT2*; fan turbine inlet temperature, *FTIT*; engine face static pressure, *PS2*; burner pressure, *PB*; and augmentor total pressure, *PT6*.

Figure 2 shows the F100 engine and the locations of its primary instrumentation sensors. The engine is controlled by a full-authority digital electronic engine control (DEEC) system that is similar to the current production F100-PW-220 engine controller. The DEEC controls the fan operating point to provide a high level of thrust while it maintains a conservative fan stall margin and avoids the maximum *FTIT* limit. The DEEC maintains the desired fan operating point by controlling corrected fan speed with *WF* and by controlling *EPR* with *AJ*. The DEEC is modified to accept PSC-commanded inputs.

The DEEC uses control schedules designed to maintain adequate stability for worst-case conditions. To accommodate a worst-case condition, a conservative amount of fan stall margin is required at all times. However, for the F100 engine, the maximum level of fan efficiency typically occurs well above the nominal operating line and near the fan stall line. Thus, the designed-in stability buffer that assures stable engine operation for worst-case conditions also inhibits more efficient operation.

Figure 3 shows a breakdown of contributions to the fan stall margin audit with and without PSC. Allowances for determining the minimum allowable stall margin are given for engine-to-engine and control tolerance variations or random effects, Reynolds number effects, worst-case inlet distortion, and afterburner transients. Because PSC was designed to operate in quasi-steady-state flight conditions with fixed throttles, the inlet distortion contribution to the stall margin audit is reduced, and the afterburner transients effect may be ignored completely. The PSC also actively calculates the location of the fan stall line with an on-line adaptive airflow estimate. By improving upon the DEEC airflow calculation and restricting maneuver and throttle to quasi-steady-state conditions, the PSC design takes advantage of the excess stall margin. Thus, the minimum

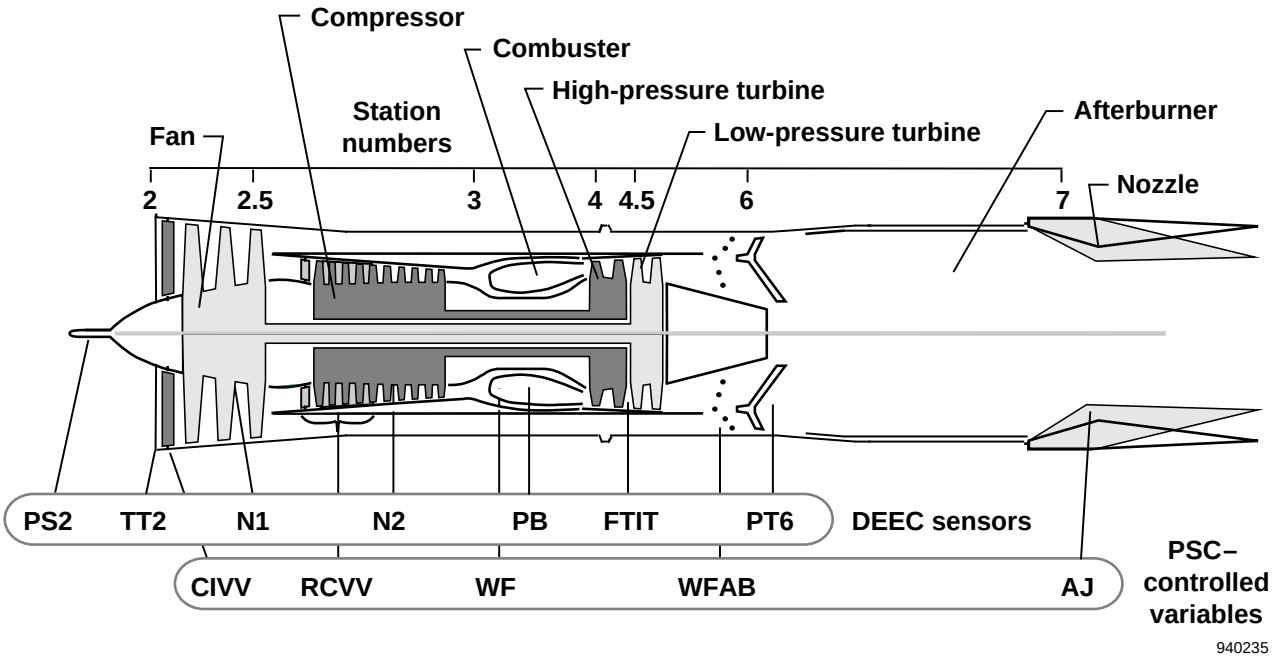

Figure 2. The F100 engine and instrumentation.

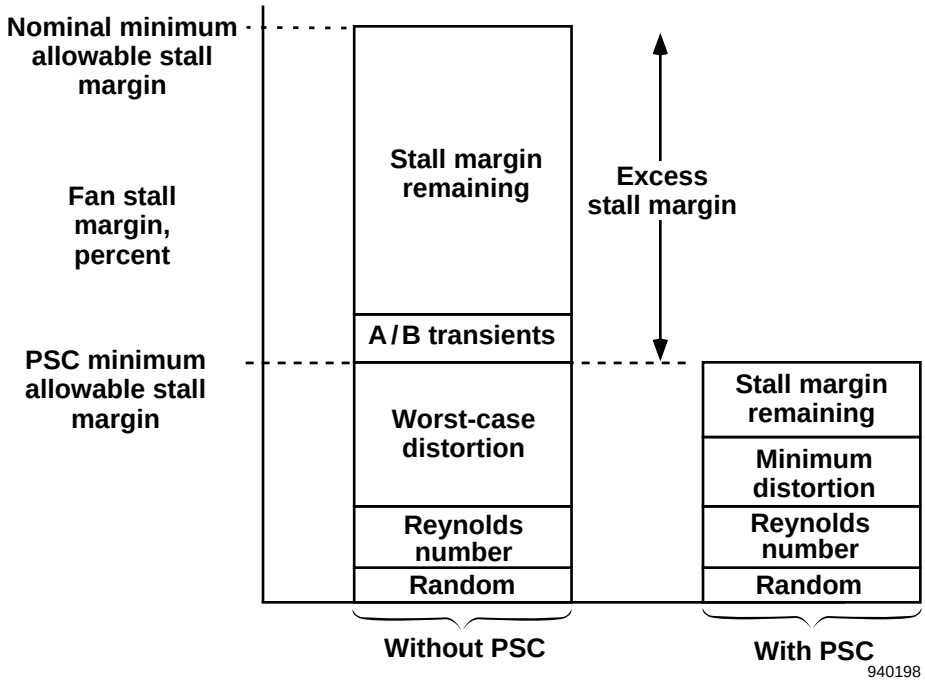

Figure 3. Relative fan stall margin audit with and without performance seeking control. Audit varies with power level angle and flight condition.

allowable stall margin is less than that of the DEEC when PSC is used.

Variable Geometry Inlet

The F-15 aircraft has two two-dimensional, three-ramp, external compression inlets which supply airflow to the PW1128 engines (fig. 4). For supersonic operation, compression is accomplished through three oblique shocks and one terminal normal shock. The F-15 aircraft has two electronic air inlet controllers (EAICs) to control the inlet variable geometry. The inlet control logic positions the cowl and third ramp to achieve adequate performance while maintaining safe operating margins. An inlet delivers high

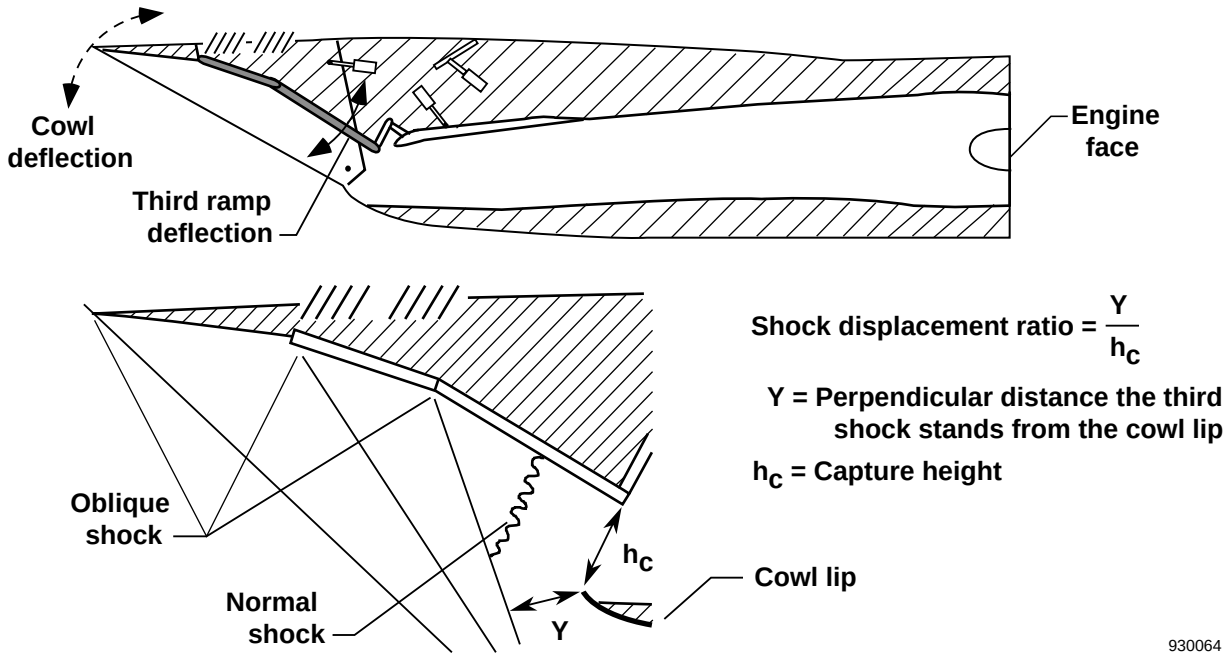

Figure 4. The F-15 variable geometry inlet.

performance when it provides for high-pressure recovery at the engine face, low airflow spillage drag, and minimum stabilator trim drag. Because the inlet is located well ahead of the center of gravity, variation in cowl position will cause a pitching moment which will be counteracted by the horizontal stabilator. Thus, the inlet is an integrated effector that couples propulsive and aerodynamic system performance. The EAIC maintains inlet stability margins by using conservative schedules to avoid encountering inlet buzz and supercritical operation. Inlet buzz is primarily a high-distortion phenomenon that occurs at low airflows. Supercritical operation occurs when the oblique shocks terminate inside of the inlet lip, and the normal shock is ingested beyond the inlet throat.

PSC Algorithm Overview

The PSC, as developed by McDonnell Douglas Aerospace (MDA), St. Louis, Missouri, and installed on the NASA F-15 HIDEC, is a model-based, adaptive algorithm that optimizes the propulsion system during quasi-steady-state operation in real-time. Information available from the onboard digital computers, such as airdata, flight control parameters, and engine measurements, is shared with the PSC software. Basically, the algorithm consists of an estimation routine to update propulsion models and an optimization routine to optimize model–predicted performance. After optimizing the models, optimal trims are applied to the propulsion system in an open-loop manner.

Figure 5 shows the three major algorithm elements as they reside in the VMS computer. These elements include the identification, modeling, and optimization components. The entire PSC algorithm is duplicated for left and right propulsion systems. No cross-communication exists between the model, identification, or optimization components. Thus, either engine is optimized independently of the other engine. The PSC trims are applied to the propulsion system approximately 5 times/sec subsonically and 2 times/sec supersonically. The reduced trim application time during supersonic operation results from the inclusion of the large inlet model. Detailed descriptions of the PSC algorithm have been reported.[2, 5, 8] Selected aspects are described in the following subsections.

Identification

A Kalman filter (Kf) provides real-time algorithm adaptability for off-nominal engine performance. Off-nominal engine performance relates to the difference between model outputs and engine measurements. To characterize these differences, the Kf identifies five CDP that represent deviations from nominal engine operation. These CDP include efficiencies for the low- and high-pressure turbine spools, incremental airflows for the low- and high-pressure compressors, and effective gas path flow area through the high-pressure turbine.[13] A separate Kf is maintained for the left and right engines, so corrections may be made for known measurement biases particular to each engine. Input to the Kf was constrained to standard DEEC measurements.

The CDP comprise a set of intermediate variables passed to the PSC integrated system model. The integrated

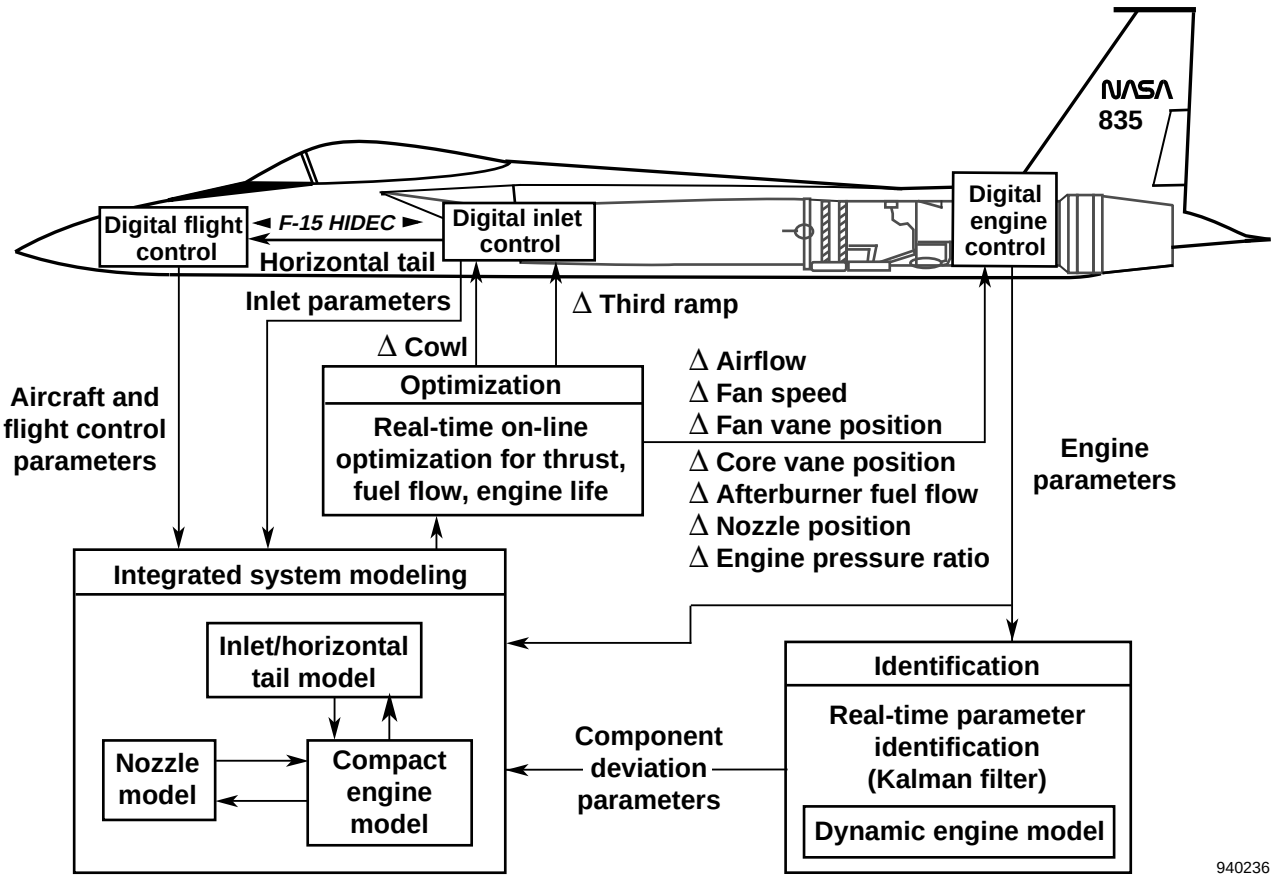

Figure 5. Performance seeking control algorithm.

system model operation is incrementally adjusted with the CDP to more accurately match measured engine operation. This adaptive feature allows for the PSC optimization to be applied to any F100 engine independent of its state of degradation.

The CDP for the nominal engine are zero by definition. Engine efficiency is not the only influence on the CDP. The CDP are sensitive to any measured difference from the nominal engine, including engine-to-engine variations, engine deterioration, measurement bias, and Reynolds number effects.[4] Because of an observability limitation within the Kf, the influence of any single effect on the CDP can not be identified.[14] This weakness is related to the limited number of measurements available from the standard DEEC and the number of CDP being estimated.

Modeling

The integrated system model consists of compact models for the engine, nozzle, and inlet. The engine model consists of a linear steady-state variable model and nonlinear model routines for effects which can not be accurately represented with the linear model, such as fan stall margin. The nozzle and inlet also use nonlinear models. With measurements and CDP as input, the models predict the current state and performance of the propulsion system. The models estimate propulsion system parameters that are not directly measurable, such as nozzle exhaust temperature, fan stall margin, percentage critical inlet mass flow, and net propulsive force, *FNP*. The integrated system model generates a linear propulsion system representation around the operating point. This linear model is needed by the optimization logic to determine system sensitivities to control inputs. A detailed description of the PSC compact models has previously been reported.[5, 9]

The optimization logic requires sensitivity information about the propulsion system. Within the algorithm, control variables are perturbed by the optimization logic and returned as input to the integrated system model to determine airframe and propulsion system sensitivities. An optimal control trim set is then determined based upon the modeled sensitivities, the constraints, and a performance index. Next, this trim set is sent to the actual inlet, nozzle, and engine. Thus, the optimal trim commands applied to the real propulsion system are based upon an optimization of the integrated system model.

Optimization

The optimization logic employs a linear programming technique to optimize the integrated system model. Four optimization modes are pilot selectable: minimum fuel at

constant thrust, maximum thrust, minimum turbine temperature at constant thrust, and rapid deceleration. Performance index and equality constraint are different for each mode. The performance indices for the four modes are total engine fuel flow, *FNP*, *FTIT*, and *FNP*, respectively. The maximum thrust mode attempts to maximize *FNP*, whereas the RDM attempts to minimize *FNP*. The maximum thrust mode and RDM do not include equality constraints. The minimum fuel and minimum turbine temperature modes are constrained to maintain a constant level of *FNP*. The controls available to the optimization logic for trimming include inlet cowl and third ramp angles, engine airflow, fan speed, fan and core variable vane angles, engine exhaust nozzle area, *EPR*, and *WFAB*.

To create the new RDM, only minor modifications to the optimization logic of the PSC algorithm were made. The two most significant additions involved a new performance index, the negative sign of *FNP*, and a minimum airflow constraint based on a newly defined inlet buzz boundary.

Flight Test Program

The initial supersonic PSC flight test program was conducted at NASA Dryden during 1992. Objectives included algorithm validation and single-engine demonstration of PSC in the F-15 supersonic flight envelope. Following the initial supersonic flight tests, the PSC algorithm was modified to optimize two engines simultaneously. The next phase of flights, known as the dual-engine supersonic PSC phase, demonstrated the effects of the PSC maximum thrust mode optimization on aircraft acceleration performance, the ability of the PSC to optimize two propulsion systems simultaneously, and the validation of the new RDM. The minimum fuel and turbine temperature modes were also tested with the dual-engine PSC.

Aircraft Acceleration Time Correction

One method used to evaluate the operation of PSC was a comparison of F-15 level acceleration times with and without PSC engaged for each mode. Using the maximum thrust mode, a significant increase in aircraft acceleration was expected. Acceleration times were expected to be unaffected by the minimum fuel and turbine temperature modes because those modes attempt to maintain the baseline *FNP*. However, several factors complicated the comparison of similar PSC-disengaged or -engaged acceleration test points.

Related PSC test points were often flown in sets of two. Because of the high rate of fuel consumption during a maximum augmented power acceleration, a large aircraft mass differential usually occurred at the start of each acceleration. The resulting inertia effects were correspondingly large. Mass-related aircraft trim drag differences were also significant.

Similar test points were normally flown on the same flight through the same air mass at an equivalent altitude to reduce the influences of changing atmospheric conditions on propulsion system operation and aircraft drag. Sometimes, flying related test points in sequence or even on the same day was not possible. This situation led to inevitably large atmospheric differences at the same altitude. Further discrepancies resulted from instances where the pilot was unable to maintain the same altitude that was flown during the first test point.

These differences in aircraft mass and atmospheric conditions made the comparison of acceleration times between related test points qualitative at best. To obtain quantitative data, a computer program was written that corrected the time-to-accelerate data from one test point to the mass, aircraft drag, and atmospheric conditions of a second, similar acceleration. A PW1128 quasi-steady-state aerothermodynamic engine model was used to correct for the effects of differences in atmospheric conditions on excess thrust. Meanwhile, a simplified performance model of the F-15 aircraft was used to accommodate changes in aircraft drag resulting from differences in altitude and aircraft mass.

To simplify the coding, the program did not account for potential energy effects resulting from altitude changes. The pilot normally flew the accelerations using an inertial flightpath reference on the head-up display, so the majority of test points had reproducible, relatively constant altitude profiles.

During the dual-engine PSC test phase, 5 accelerations at an altitude of 30,000 ft and 4 accelerations at an altitude of 45,000 ft were flown with PSC disengaged. Because PSC trims were not sent to the engines and inlets, theoretically the accelerations at the same altitude would overlay one another once corrected for mass and atmospheric differences. This theory was investigated to verify the proper operation of the correction code, and the correction program performed well. At an altitude of 45,000 ft, there was a 24.4 percent (34.1 sec) variation in the time to accelerate from Mach 0.8 to Mach 2 before correction, and only 1.4 percent (1.9 sec) afterwards. At an altitude of 30,000 ft, the variation was 15.8 percent (14.1 sec) before and 3.4 percent (3.0 sec) after correction from Mach 0.6 to Mach 1.6.

The test points presented later in this paper were flown back-to-back through the same air mass, essentially eliminating the correction errors associated with atmospheric deviations. Thus, the program corrected mainly for inertia effects for these points. As such, the error bands associated with the corrected time-to-accelerate data presented later should be less than 1.4 percent at an altitude of 45,000 ft and 3.4 percent at an altitude of 30,000 ft.

Results and Discussion

Test results of using the maximum thrust, minimum fuel, minimum turbine temperature, and rapid deceleration modes are discussed in the following subsections. The maneuvers were designed to evaluate PSC system operation and overall performance benefits.

Maximum Thrust Mode

The PSC maximum thrust mode improves aircraft acceleration performance by maximizing *FNP* or, equivalently, the combined quantity of engine net thrust less propulsion-related drag. Net thrust increases come primarily from the ability to operate the inlet and engine closer to operating limits and optimum conditions. For instance, the minimum operating limits for fan stall margin (fig. 3) and inlet shock displacement ratio are lower when PSC is applied. Propulsion-related drag, as accounted for in the PSC models, includes incremental drag caused by off-schedule inlets, nozzles, and stabilator. Reductions in drag come from model predictions of where the local minimum lies. In general, net thrust increases contribute more to the PSC maximum thrust mode than trim drag reductions do. The mode engages at either a military-rated or a maximum afterburner (A/B) power setting.

Figure 6 presents results from a single test point demonstration of the PSC maximum thrust mode. Comparison data of two accelerations performed at an altitude of 45,000 ft from Mach 0.9 to Mach 2 with and without use of the PSC maximum thrust mode are plotted. The runs were completed back-to-back and through the same air mass to minimize the effects of such outside influences on the experiment as atmospheric deviations. To further produce a valid comparison, the acceleration times were corrected for weight and temperature differences. With PSC engaged, the acceleration time was reduced by 14.8 sec or 8.5 percent from the baseline acceleration time (fig. 6(a)).

Figure 6(b) shows the percentage difference in *FNP* between the runs with and without PSC for the left and right engines. The *FNP* gains trend from near 10 percent subsonically to 2 percent or less in the mid-supersonic range. Approaching the Mach 2 condition, *FNP* gains increase to approximately 6 percent.

The manner in which the engines are optimized over the Mach 0.9 to Mach 2 range is typical for the maximum thrust mode. Figures 6(c) and 6(d) show the primary engine controls, *EPR* and airflow. For the subsonic and supersonic region below Mach 1.8, the *EPR* trims greatly contribute to increasing *FNP*. Above Mach 1.8, airflow uptrims command the majority of the *FNP* increase. Subsonically, the engine is driven to the minimum allowable fan stall margin. Supersonically, the inlets are driven to the maximum allowable airflow. In addition, PSC trims caused the *FTIT* to operate at its maximum limit for the entire acceleration. The differences in *FNP* increases between the left and right engines may be explained by the fact that the right engine nominally operates closer to the maximum *FTIT*. Thus, less *FTIT* margin exists to be used for increased *FNP*.

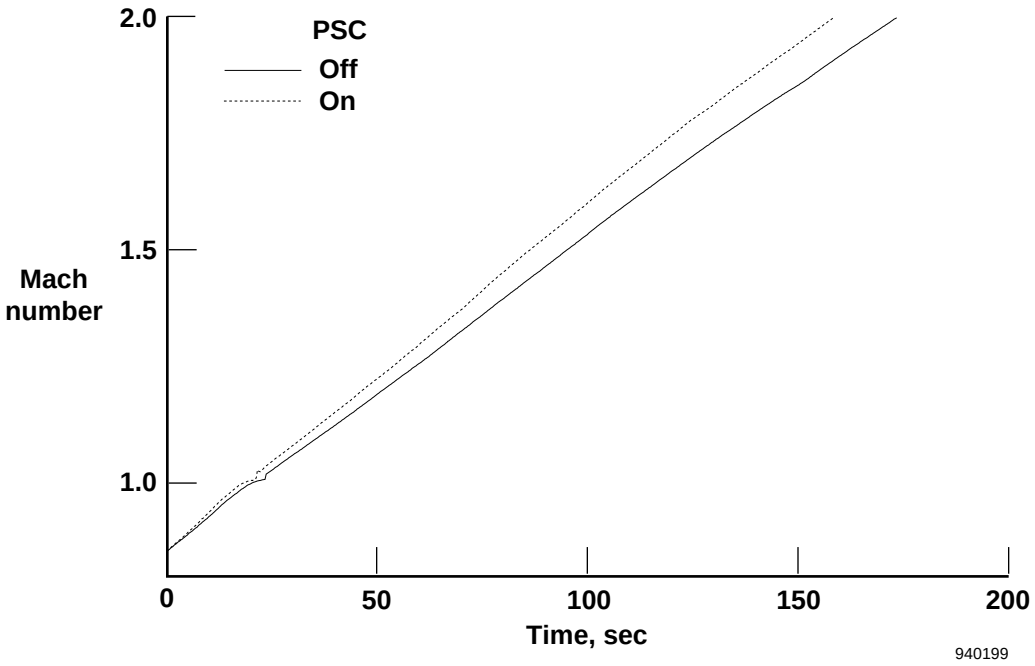

(a) Acceleration time with and without performance seeking control.

Figure 6. Maximum thrust mode evaluation for a maximum afterburner acceleration at an altitude of 45,000 ft.

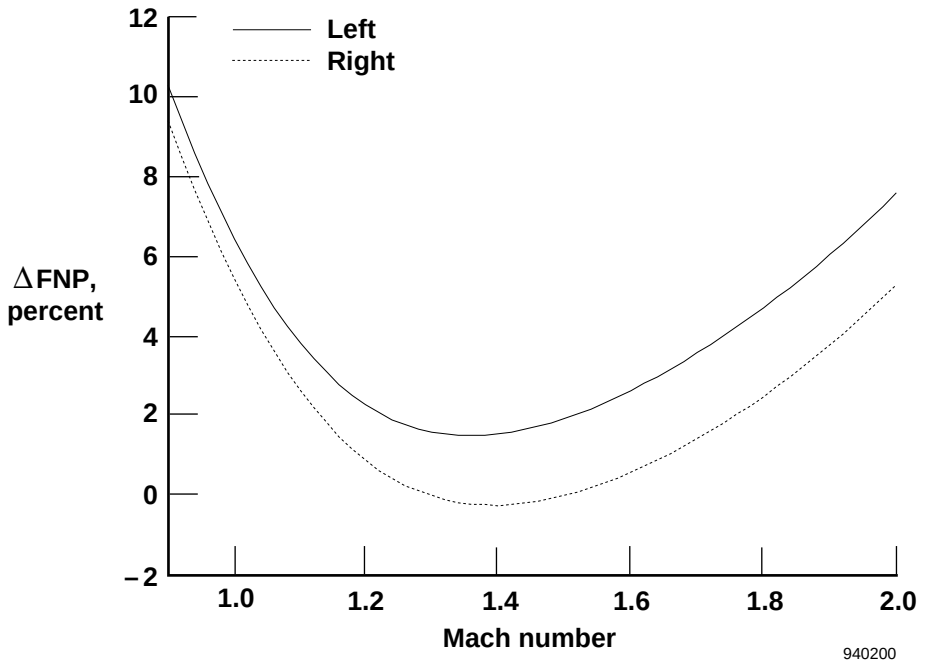

(b) Percentage of net propulsive force increase with performance seeking control.

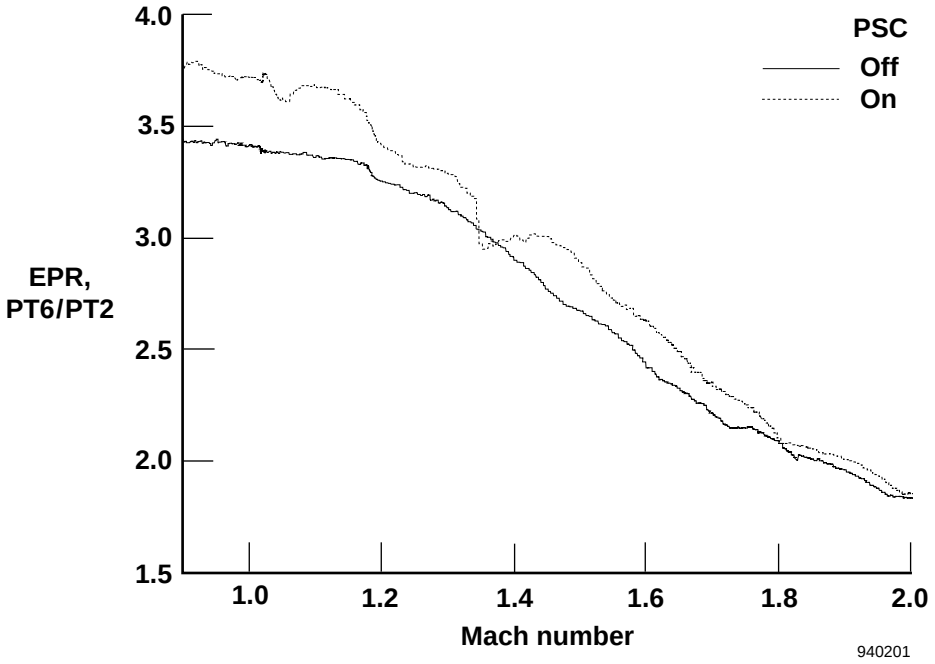

(c) Left engine pressure ratio comparison with and without performance seeking control.

Figure 6. Continued.

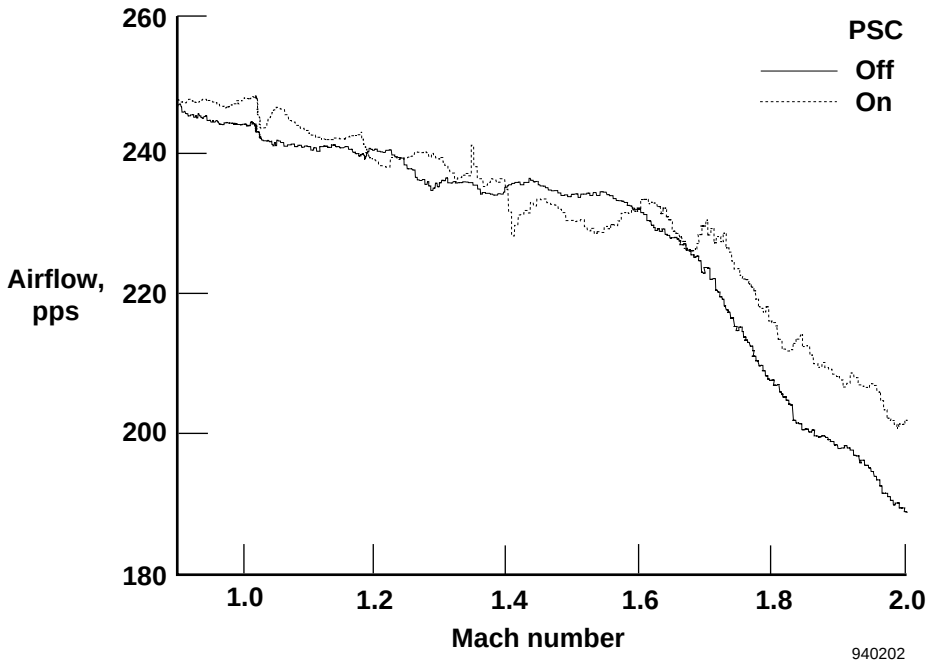

(d) Left engine afterflow comparison with and without performance seeking control.

Figure 6. Concluded.

Minimum Fuel Mode

The PSC minimum fuel mode effectively optimizes thrust-specific fuel consumption, *TSFC*, by minimizing core and afterburner engine fuel flow while maintaining *FNP*. Supersonically, the two ways by which PSC achieves lower *TSFC* are by either lessening the net thrust required for level cruise or by trading fuel flow between the more efficient engine core and the less efficient afterburner. As trim drag is reduced, so is the net thrust requirement. This reduction allows for a cutback in total engine fuel flow. However, in all cases, the primary benefits of the minimum fuel mode have been observed to be from the tradeoff between *WF* and *WFAB*. This result is not surprising given that the engine core is significantly more efficient than the afterburner in converting fuel flow into thrust. The afterburner may be downtrimmed by increasing the net thrust produced by the engine core. This core net thrust is derived primarily by adding fuel. To a lesser degree, net thrust increases can also be obtained by trimming the variable vanes and inlet ramps. This mode is operational for any fixed throttle position.

A cruise test of the minimum fuel mode was conducted at an altitude of 30,000 ft and at Mach 1.5. Figures 7(a) and 7(b) show time histories of left and right engine *FNP* and *TSFC*. The PSC optimization was engaged after 24 sec of comparison data were collected. The left and right engines were closely matched in *FNP* and *TSFC* for the duration of the test. At approximately 65 sec, PSC commanded a sharp reduction in right engine *WFAB*. This reduction is evident in the *FNP* and *TSFC* traces, but the *FNP* is recaptured rapidly. In addition, steady-state is attained for approximately 10 sec before the end of the cruise test. Based on the 24 sec period before engaging PSC and the final 10 sec of steady-state data, left engine *TSFC* was reduced by approximately 9.2 percent, and right engine *TSFC* decreased by 9.5 percent.

Figures 7(c) and 7(d) show the dramatic comparison of the engine core to afterburner fuel flows. For the left engine, *WF* is uptrimmed by just 680 pph, which allows the *WFAB* to be cut by 3230 pph. The right engine fuel flow is trimmed in the same manner. The right engine transient at 65 sec is evident in the *WFAB* trace, indicating that an afterburner segment was shut off.

Minimum Turbine Temperature Mode

The PSC minimum turbine temperature mode minimizes the measured *FTIT* while maintaining *FNP*. The *FTIT* is primarily affected by *WF* and *TT2*. In turn, the *TT2* depends on flight condition. Because PSC does not control flight condition, the *WF* is the only primary control. In general, *WF* is directly proportional to the turbine temperature. Thus, at a fixed flight condition, the PSC minimum turbine temperature mode downtrims *WF* to achieve a cooler turbine. However, reducing *WF* causes net thrust to be lost. To compensate for this loss, PSC adjusts the inlet and nozzle to reduce propulsion-related trim drag, effectively decreasing the power required for level cruise flight. This mode operates at all throttle settings. However, unlike the minimum fuel mode, the minimum turbine temperature mode does not command *WFAB*.

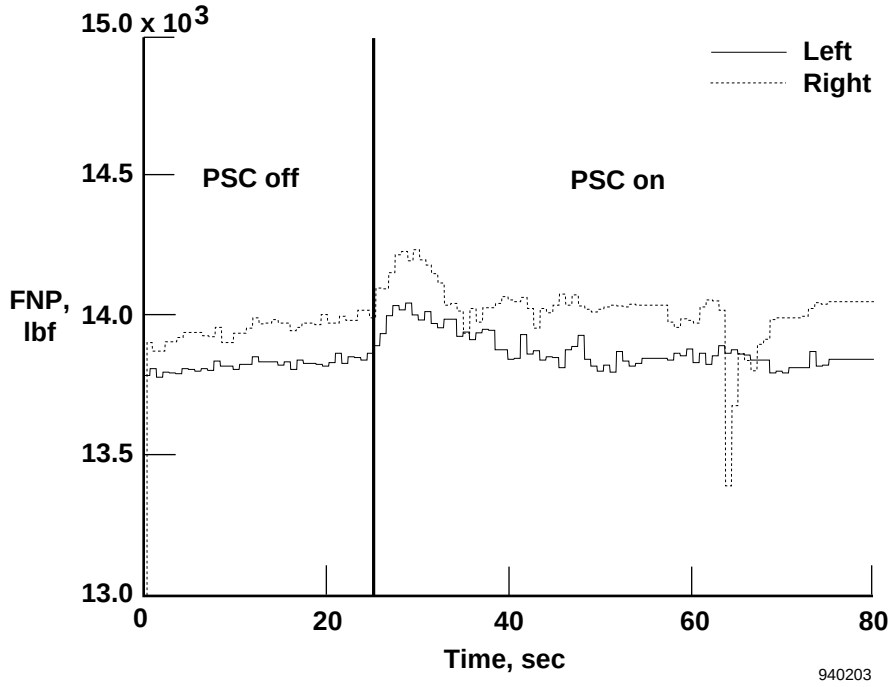

(a) Net propulsive force.

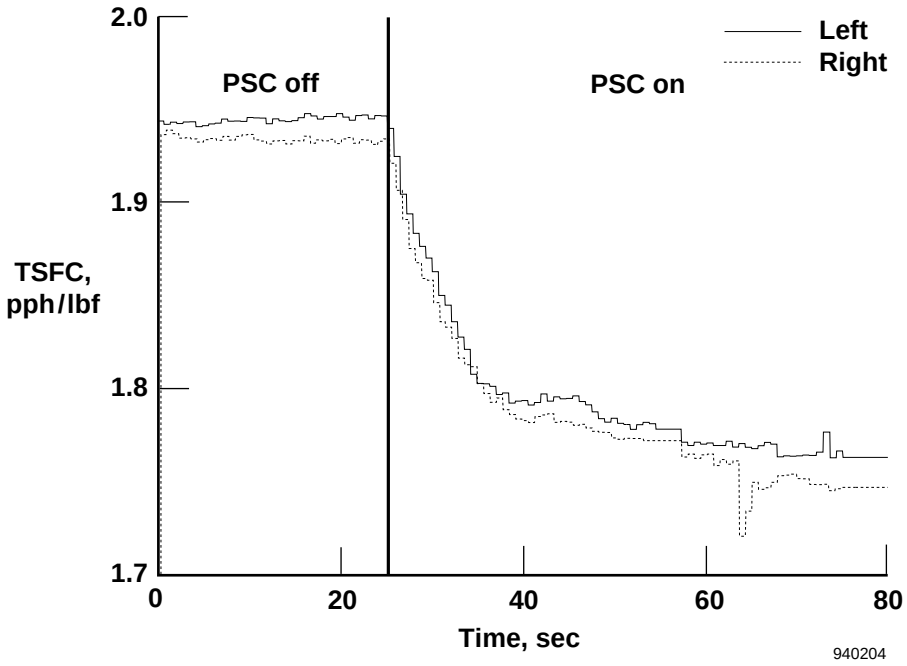

(b) Thrust-specific fuel consumption.

Figure 7. Minimum fuel mode test results for a partial afterburner cruise at Mach 1.5 and an altitude of 30,000 ft.

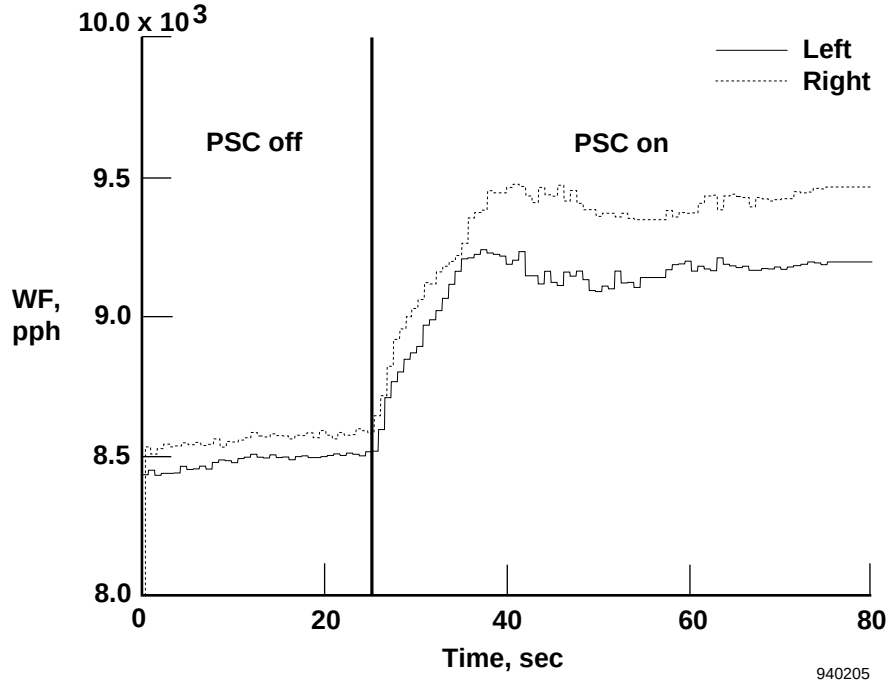

(c) Engine core fuel flow.

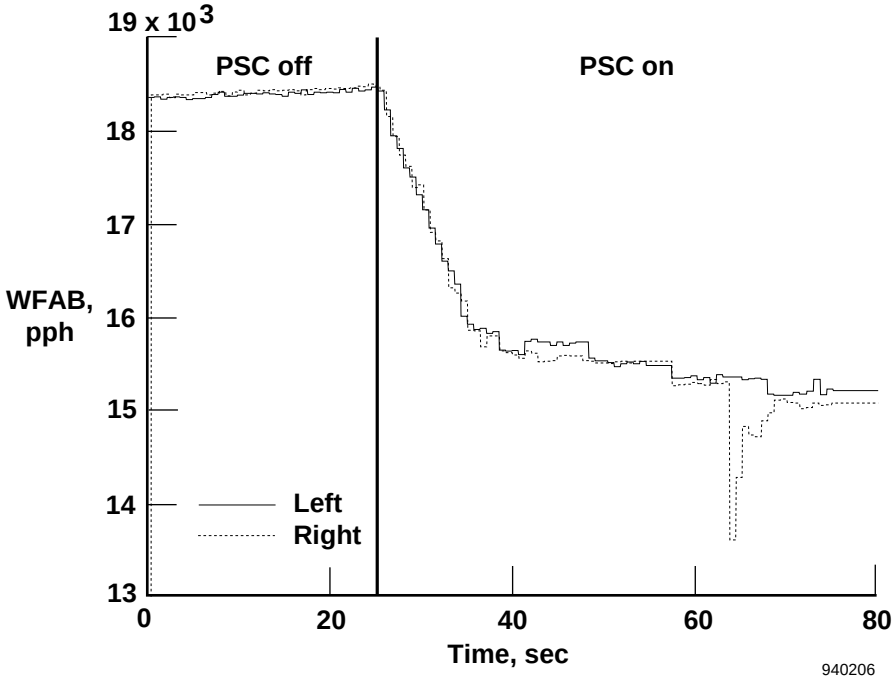

(d) Afterburner fuel flow.

Figure 7. Concluded.

The minimum turbine temperature mode was tested during a supersonic cruise at an altitude of 40,000 ft with partial afterburner power at Mach 1.8. Figure 8(a) shows that 21 sec of comparison data were collected before PSC was engaged. Upon engaging PSC, the optimization logic sets a reference value of *FNP* to be used as the equality constraint throughout the cruise maneuver. By incorrectly estimating the effect of its model-based optimal trims on *FNP,* the PSC algorithm produces some unexpected transients in *FNP* and *FTIT,* particularly on the left engine.

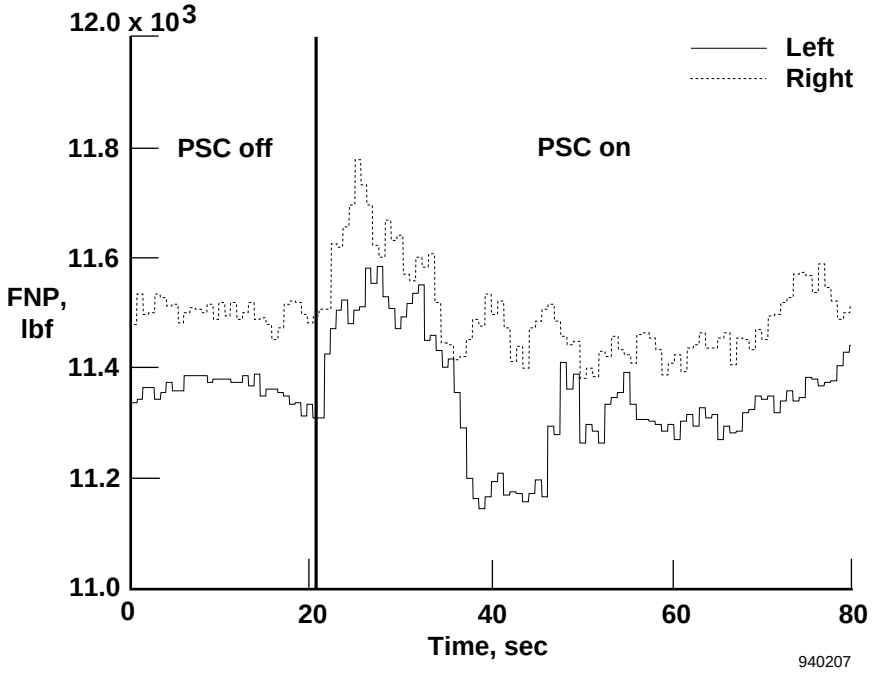

(a) Net propulsive force.

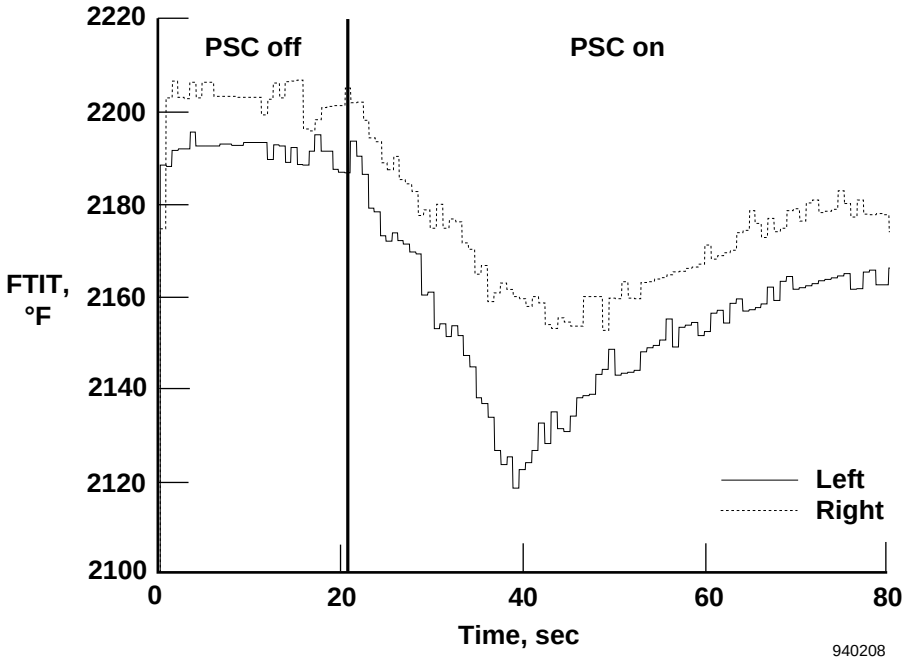

(b) Fan turbine inlet temperature.

Figure 8. Minimum turbine temperature mode evaluation for a partial afterburner cruise at Mach 1.8 and an altitude of 40,000 ft.

Left and right *FNP* temporarily violate the equality constraints during the transients, but eventually both return to within 50 lbf of the reference levels.

During the first 20 sec of applying trims, *FTIT* was reduced by 70 and 50 °F for the left and right engines, respectively (fig. 8(b)). However, that level is unsustainable, as evidenced in the *FNP* and *FTIT* traces. After nearly 50 sec of PSC trim applications, *FTIT* has either reached or neared steady-state, and the algorithm has stabilized. Based on the first 10 and last 20 sec of data, PSC reduces *FTIT* by 27 and 25 °F for the left and right

engines, respectively. To put these temperature reductions in perspective based solely on temperature effects, every 70 °F reduction doubles turbine life.[8]

Figures 8(c) to 8(e) show how the *FTIT* was reduced by PSC during the cruise test. The combined reductions of nozzle drag, stabilator trim drag, and inlet drag for both engines totaled between 300 and 400 lbf. Figure 8(c) shows the net drag reduction. The drag reduction allowed for the net thrust to also be cut back, primarily by the downtrim in *WF*. Left and right engine *WF* decreased by 325 and 305 pph, respectively. Note the strong correlation of shape even during the transient of the fuel flow and *FTIT* traces.

Rapid Deceleration Mode

Several instances exist where it is desirable to increase the rate of an aircraft's supersonic deceleration. During in-flight emergencies, such as a loss of pressurization at supersonic speeds, the ability to rapidly decelerate allows the aircraft to reach the low altitude and subsonic domain quickly. In this domain, controllability increases, and mission abort and egress options multiply. For military aircraft flying supersonic intercept missions, rapid deceleration gives the pilot increased control when engaging the adversary. Reducing infrared signature by lowering engine exhaust temperature and slowing more rapidly may also be desired.

The standard F-15 aircraft uses a military power engine lockup schedule to maintain maximum airflow when the aircraft is above Mach 1.4 even when the throttles are brought below military power. The power lockup prevents a low frequency, high-amplitude inlet resonance phenomenon known as buzz. Buzz occurs when inlet airflow decreases below a Mach number-dependent critical value. Driven by the oscillation of the shock system, buzz is very uncomfortable for the pilot and potentially damaging to the inlet structure.

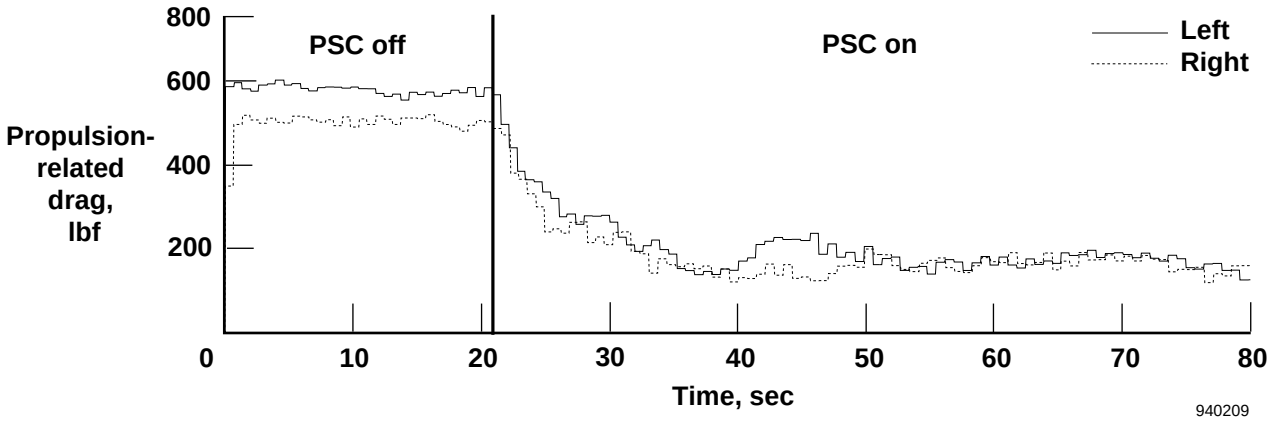

(c) Propulsion-related drag.

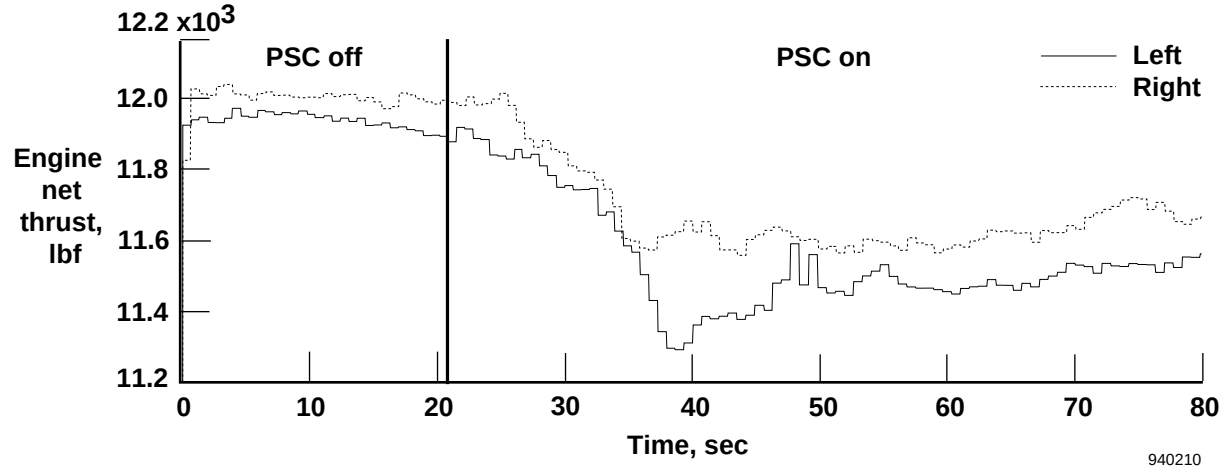

(d) Engine net thrust.

Figure 8. Continued.

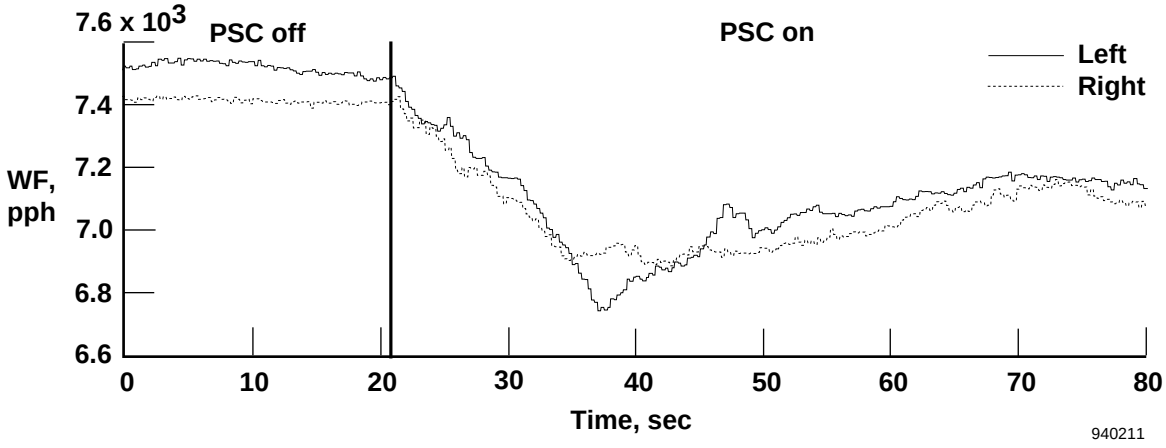

(e) Engine core fuel flow.

Figure 8. Concluded.

As the F-15 aircraft decelerates below Mach 1.4, the engine control permits engine airflow to decrease because the risk of encountering buzz declines with decreasing speed. The engine control schedules the airflow primarily as a function of Mach number. There is no direct closed-loop, measurement-based avoidance of buzz.

The F-15 engine controls create a large buffer between the scheduled engine airflow and the buzz-inducing airflow while in the lockup schedule. This buffer precludes the occurrence of buzz caused by varying day conditions and engine and inlet differences between aircraft. However, the buffer creates a longer supersonic deceleration time than would result if the engine operated within a tighter tolerance of the airflow buzz boundary.

The PSC RDM bypassed the DEEC military power lockup schedule and drove the propulsion system to an even lower *FNP* value. The RDM uses logic similar in operation to that of the maximum thrust mode. However, in this mode, PSC drives the *FNP* to its minimum allowable value. The primary constraint is minimum engine airflow. This constraint is a function of Mach number and was selected to permit improved tracking of the airflow buzz boundary while still providing enough margin to avoid buzz. MDA reanalyzed F-15 wind tunnel data and produced a more accurate minimum airflow constraint definition. The revised definition allowed the airflow to be further downtrimmed with more confidence.

The inlet ramps were reconfigured by RDM to increase inlet and trim drag, using ramp position–drag relationships and built-in shock ingestion prevention logic. The combined decreased thrust and increased drag configuration brought the aircraft to subsonic speeds much more quickly than is possible with the standard military power lockup schedule.

Figure 9 presents the benefits of the RDM in tests performed at an altitude of 45,000 ft. The test setup consisted of accelerating the aircraft at maximum augmentation to a speed approximately Mach 0.2 faster than the desired initiating Mach number then bringing both throttles to the idle position. In decelerating to the starting Mach number, the PSC algorithm was given time to stabilize. The pilot then engaged PSC. Engine thrust was reduced, the inlets were reconfigured, and the plane was allowed to decelerate straight and level to low supersonic speed. The pilot then disengaged the mode, and the engines and inlets were returned to their normal operating schedule. For comparison purposes, a second deceleration was also flown straight and level at each test altitude without the use of the PSC algorithm. The speed brake was stowed for the example presented.

The pilot engaged PSC at Mach 1.98 and ended its use at Mach 1.1. Using RDM, deceleration time was reduced by 50 percent, or from 139 to 69.5 sec (fig. 9(a)). Figure 9(b) presents the change in component force and drag resulting from the use of RDM. Net thrust was greatly reduced, primarily as a result of the reduction in engine airflow. Inlet drag was substantially increased by moving the inlet shock system further open, thereby increasing airflow spillage. Trim drag also increased as the inlet cowl was rotated upwards. The change in nozzle drag was minimal. Figure 9(c) compares engine fuel flow as a function of Mach number for both test points and shows the large reduction that occurs with RDM engaged (for example, 62 percent at Mach 1.4). A correspondingly large decrease in engine operating temperature also occurs (fig. 9(d)). The *FTIT* is compared for both test points. For example, *FTIT* is reduced by 560 °F or 33 percent at Mach 1.4 with PSC engaged.

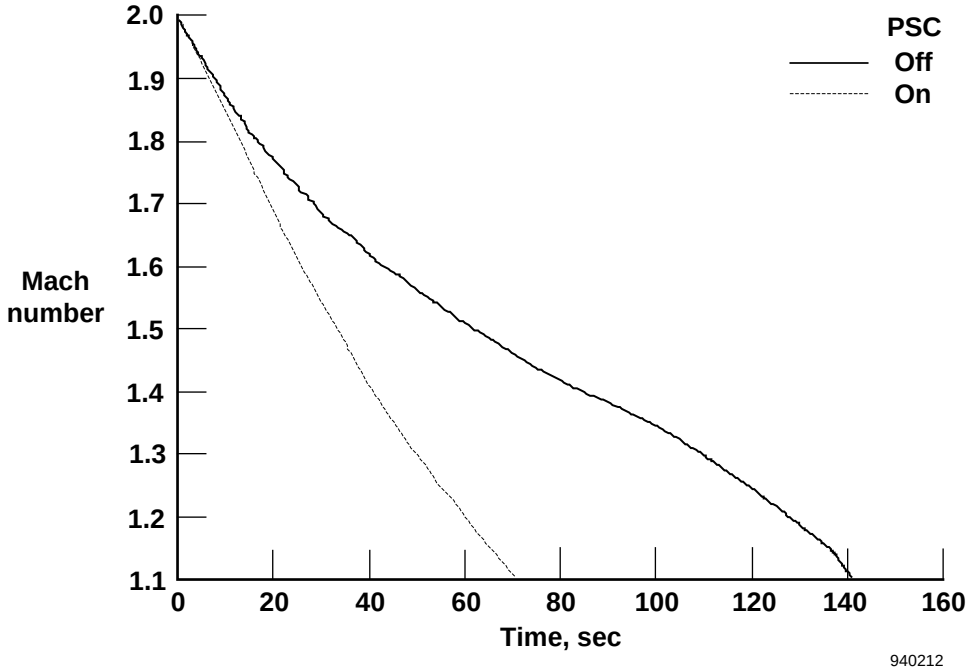

(a) Deceleration time.

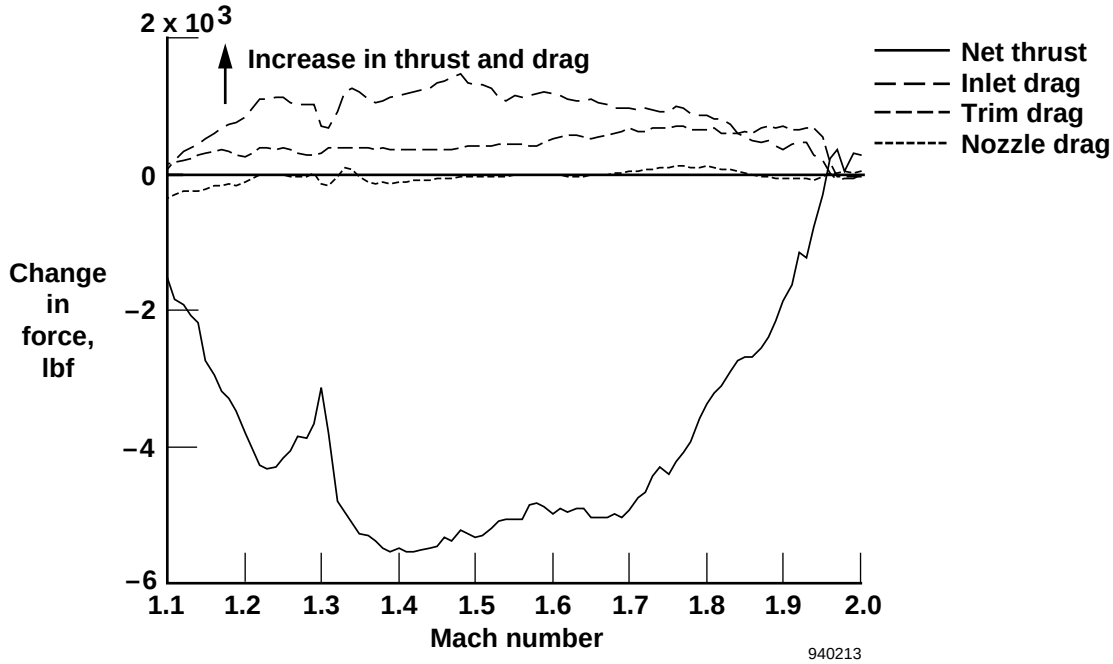

(b) Thrust and drag.

Figure 9. Rapid deceleration mode evaluation for an idle power setting deceleration at an altitude of 45,000 ft with and without performance seeking control .

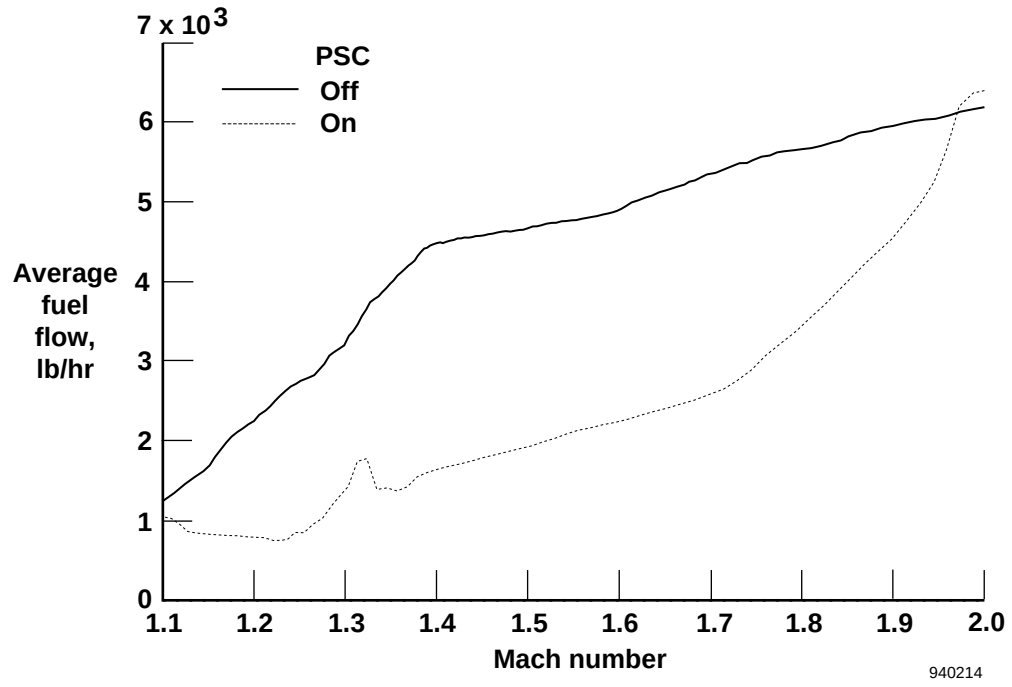

(c) Total fuel flow.

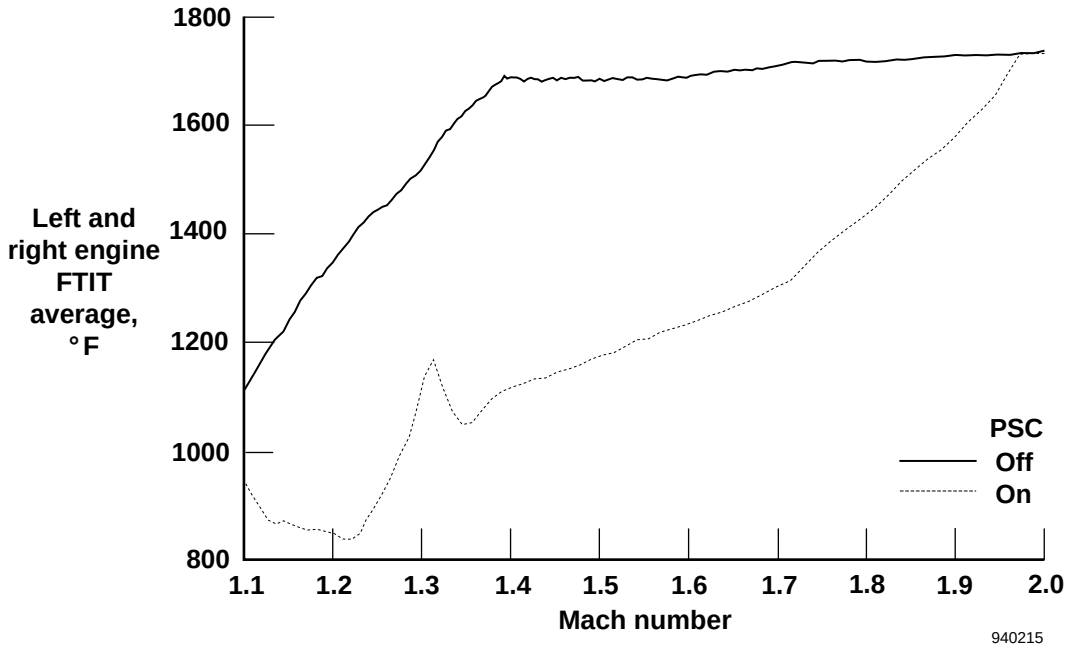

(d) Fan turbine inlet temperature.

Figure 9. Concluded.

The time-to-decelerate data were corrected for weight and trim drag differences between the PSC off and on decelerations. No inlet buzz problems occurred using RDM. The RDM successfully demonstrated the benefits of integrating the engine control with a thrust calculation algorithm and off-nominal inlet scheduling. Flexibility of the PSC algorithm in effectively accommodating different performance goals was also proven. In this case, the antithesis of the maximum thrust mode drove the propulsion system to a minimum force value. This value was constrained primarily to an accurate minimum airflow boundary.

Concluding Remarks

Flight testing of a model-based, adaptive control algorithm was performed on a NASA F-15 aircraft with integrated engine and airframe control. This algorithm, Performance Seeking Control (PSC), seeks to improve upon the advanced engine control system by applying real-time adaptation to the flight-measured article.

Initial flight tests performed algorithm validation and single-engine demonstration of PSC in the supersonic flight envelope. The last series of flight tests concentrated on the dual-engine application of PSC at supersonic flight conditions, demonstrating how PSC optimizes two systems independently and simultaneously. The tests also validated the new rapid deceleration mode (RDM).

The PSC algorithm consists of an estimation routine to update propulsion models and an optimization routine to optimize the model–predicted performance. An integrated system model predicts the current state and performance of the propulsion system, using a Kalman filter to adapt off-nominal engine performance to real-time and estimating the parameters that can not be measured. The optimal control trim set is based upon this integrated system model, then is sent to the actual propulsion system. The PSC algorithm is duplicated for left and right propulsion systems, allowing one engine to be optimized independently of the other engine.

A linear programming technique optimizes this integrated system model, allowing pilot selection of four optimization modes: maximum thrust, rapid deceleration, minimum fuel, and minimum turbine temperature. Testing of these modes has been concluded. Overall engine performance improvements were demonstrated for the single-engine application in subsonic and supersonic flight testing. Aircraft performance improvements were directly measurable for dual-engine supersonic flight. The modes were evaluated to illustrate the manner in which PSC achieves its results in the supersonic envelope.

Accelerations and decelerations were flown to test the PSC maximum thrust mode and RDM, respectively. During the maximum thrust mode acceleration testing at an altitude of 45,000 ft, the PSC commanded optimal inlet and engine uptrims. The PSC model estimated the left and right propulsion system produced an average of 4 percent more thrust than the baseline. These estimated improvements are evidenced by the measured 8.5 percent reduction in acceleration time from Mach 0.9 to Mach 2. The application of the PSC RDM led to quicker decelerations. At an altitude of 45,000 ft, time to decelerate from Mach 2 to Mach 1.1 decreased by 50 percent.

The results from the minimum fuel and turbine temperature modes showed that PSC can substantially improve thrust-specific fuel consumption (*TSFC*) and be used to extend engine life. Cruise testing of the PSC minimum fuel and turbine temperature modes demonstrated the ability of the PSC algorithm to hold net propulsive force constant while minimizing *TSFC* or fan turbine inlet temperature, *FTIT*. As predicted, PSC held flight condition by controlling model-estimated thrust to a constant level for both modes. At Mach 1.5 and an altitude of 30,000 ft, *TSFC* was reduced by over 9 percent for both sides of the propulsion system primarily by reducing afterburner fuel flow requirements. A minimum turbine temperature mode test at Mach 1.8 and an altitude of 40,000 ft resulted in an *FTIT* decrease of 25 °F or more for both engines while holding a constant thrust and flight condition. Because the baseline engine operates on the maximum *FTIT* limit at this flight condition, 25 °F reduction translates to increased engine life.

References

[1]Yonke, W.A., Terrell, L.A., and Myers, L.P., "Integrated Flight/Propulsion Control: Adaptive Engine Control System Mode," AIAA-85-1425, July 1985.

[2]Smith, R.H., Chisholm, J.D., and Stewart, J.F., "Optimizing Aircraft Performance With Adaptive, Integrated Flight/Propulsion Control," *Journal of Engineering for Gas Turbines and Power*, vol. 113, Jan. 1991, pp. 87–94.

[3]Tich, Eric J., Shaw, Peter D., Berg, Donald F., Adibhatla, Shrider, Swan, Jerry A., and Skira, Charles A., "Performance Seeking Control for Cruise Optimization in Fighter Aircraft," AIAA-87-1929, June 1987.

[4]Orme, John S. and Gilyard, Glenn B., *Subsonic Flight Test Evaluation of a Propulsion System Parameter Estimation Process for the F100 Engine*, NASA TM-4426, 1992.

[5]Gilyard, Glenn B. and Orme, John S., *Subsonic Flight Test Evaluation of a Performance Seeking Control Algorithm on an F-15 Airplane*, NASA TM-4400, 1992.

[6]Chisholm, J.D., "In-Flight Optimization of the Total Propulsion System," AIAA-92-3744, July 1992.

[7]Conners, Timothy R., *Thrust Stand Evaluation of Engine Performance Improvement Algorithms in an F-15 Airplane*, NASA TM-104252, 1992.

[8]Lambert, H.H., Gilyard, G.B., Chisholm, J.D., and Kerr, L.J., *Preliminary Flight Evaluation of an Engine Performance Optimization Algorithm*, NASA TM-4328, 1991.

[9]Orme, John S. and Gilyard, Glenn B., *Preliminary Supersonic Flight Test Evaluation of Performance Seeking Control*, NASA TM-4494, 1993.

[10]Nobbs, S.G., Jacobs, S.W., and Donahue, D.J., "Development of the Full-Envelope Performance Seeking Control Algorithm," AIAA-92-3748, 1992.

[11]Landy, Robert, "F-15 Aircraft and Inlet Description," *Highly Integrated Digital Electronic Control Symposium*, NASA CP-3024, 1987, pp. 54–64.

[12]Spencer, C.R., "Engine Description and DEEC," *Highly Integrated Digital Electronic Control Symposium*, NASA CP-3024, 1987, pp. 66–80.

[13]Luppold, R.H., Roman, J.R., Gallops, G.W., and Kerr, L.J., "Estimating In-Flight Engine Performance Variations Using Kalman Filter Concepts," AIAA-89-2584, July 1989.

[14]España, Martín D. and Gilyard, Glenn B., *On the Estimation Algorithm Used in Adaptive Performance Optimization of Turbofan Engines*, NASA TM-4551, 1993.